# A Solid-State NMR Study of Tungsten Methyl Group Dynamics in $[W(\eta^5\text{-}C_5Me_5)Me_4][PF_6]$

**Douglas C. Maus,[#] Valérie Copié,[§] Boqin Sun,[#] Janet M. Griffiths,[#,‡] Robert G. Griffin,*[,#] Shifang Luo,[&] Richard R. Schrock,* Andrew H. Liu,[∞] Scott W. Seidel, William M. Davis, and Andreas Grohmann[†]**

*Contribution from the Francis Bitter Magnet Laboratory and Department of Chemistry, Massachusetts Institute of Technology, Cambridge, Massachusetts 02139*

*Received January 23, 1996*[⊗]

**Abstract:** We report the results of Magic Angle Spinning (MAS) $^{13}C$ and static $^{2}H$ NMR studies of the dynamics of the methyl groups coordinated to tungsten in $[WCp^*Me_4][PF_6]$ ($Cp^* = \eta^5\text{-}C_5Me_5$). The temperature-dependent broadening of the axial methyl $^{13}C$ line can be ascribed to interference between $^{1}H$ decoupling and methyl motion when the motional rate and decoupling nutation frequency are comparable. This proposal is consistent with the absence of broadening in the $^{2}H$ labeled compound and the motional rate constants inferred from $^{2}H$ NMR lineshape and $T_1$ studies, which range from $10^7$ $s^{-1}$ at 25 °C to $10^3$ $s^{-1}$ at −125 °C. The measured barrier to axial methyl hopping (26 kJ/mol) is among the highest reported to date. An X-ray crystal study of $[W(\eta^5\text{-}C_5Me_4Et)Me_4][PF_6]$ reveals no evidence (in terms of the core geometry) for an agostic interaction in either the axial methyl group or the equatorial methyl groups.

## Introduction

NMR has been employed extensively to investigate dynamic processes in liquids and solids because of the wide range of kinetic time scales that are accessible. Usually these studies involve analysis of line shapes or relaxation times, which directly yield information concerning the rates and mechanisms of motion. However, in many cases dynamic information presents itself in unusual and unexpected ways. We discuss such a case here, where the interference of 3-fold methyl motion and $^{1}H$ decoupling conspire to broaden solid-state Magic Angle Spinning (MAS) $^{13}C$ lines. We note that this interference effect, which results in substantial loss of signal intensity in $^{13}C$ MAS spectra, is postulated to explain spectral intensity losses in a diverse array of situations where molecular diffusion is present, for example, in spectra of peptides and proteins diffusing in a bilayer membrane,[1−4] in small peptides where there is two or three site motion of a sidechain,[5] etc. This phenomenon is thus ubiquitous in solid-state MAS NMR. However, in general (as in the case of the membrane protein and peptide spectra) the signal-to-noise ratio was insufficient to unambiguously establish the origin of the intensity losses. The investigation described here utilizes a combination of $^{2}H$ quadrupole echo spectra to determine the rates of motion and subsequently to calculate the effect of this motion on the decoupling in $^{13}C$ MAS spectra. Since the sample is a small molecule, isotopic labeling is relatively facile, and the signal-to-noise therefore sufficient for detailed mechanistic studies.

$[WCp^*Me_4][PF_6]$ ($Cp^* = \eta^5\text{-}C_5Me_5$)[6] is an appropriate molecule to study for several additional reasons. First, it is the only $M(\eta^5\text{-cyclopentadienyl})L_4$ complex with a trigonal-bipyramidal "piano stool" structure instead of a square-pyramidal structure.[7] For example, $WCp^*Me_4$, which is formed upon addition of one electron to $[WCp^*Me_4]^+$, is likely to have a square-pyramidal structure on the basis of an X-ray structure of a closely analogous species.[6] The electrochemistry of $[WCp^*Me_4]^+$ and $WCp^*Me_4$ consequently is strongly dependent on the time scale of the electrochemical experiment,[6] as elucidated in detail in a recent study by Lerke and Evans.[8] Second, $[WCp^*Me_4]^+$ readily loses a proton to yield unstable $WCp^*Me_3(CH_2)$ in which the two methylene protons are grossly inequivalent, presumably as a consequence of an agostic[9] interaction of one of the methylene C−H bonds with the metal, a characteristic of some alkylidene complexes of early transition metals.[10] Recently, Green and co-workers have claimed, on the basis of variable-temperature studies of partially deuterated $[WCp^*Me_4]^+$, that the *equatorial methyl groups* in trigonal-bipyramidal $[WCp^*Me_4]^+$ are also agostic, i.e., that at any given instant one of the nine C−H bonds is interacting weakly with the metal. "Activation" of an α hydrogen through an α agostic interaction could conceivably be the source of the relatively high acidity of $[WCp^*Me_4]^+$ and its ready deprotonation by triethylamine. Finally, solution NMR studies indicated that trigonal-bipyramidal $[WCp^*Me_4]^+$ is fluxional; the "equatorial" and "axial" methyl groups exchange rapidly on the NMR time scale (rate

[#] Francis Bitter Magnet Laboratory, MIT.
[‡] Present address: Department of Chemical Engineering, MIT, Cambridge, MA.
[§] Present address: National Institute of Dental Research, NIH, Bethesda, MD.
[&] Present address: Exxon Research & Engineering Company, Clinton Township, Route 22 E., Annandale, NJ 08801.
[†] Present address: Institute for Inorganic Chemistry, Egerland Str. 1, 91058 Erlangen, Germany.
[∞] Present address: E. I. duPont de Nemours and Company, Jackson Laboratory, New Jersey.
[⊗] Abstract published in *Advance ACS Abstracts,* June 1, 1996.

(1) Smith, S. O.; Palings, I.; Copié, V.; Raleigh, D. P.; Courtin, J.; Pardoen, J. A.; Lugtenburg, J.; Mathies, R. A.; Griffin, R. G. *Biochemistry* **1987**, *26*, 1606.
(2) Sefcik, M. D.; Schaefer, J.; Stejskal, E. O.; MacKay, R. A.; Ellena, J. F.; Dodd, S. W.; Brown, M. F. *Biochem. Biophys. Res. Commun.* **1983**, *114*, 1048.
(3) Lewis, B. A.; Harbison, G. S.; Herzfeld, J.; Griffin, R. G. *Biochemistry* **1985**, *24*, 4671.
(4) Lee, C. W. B. Ph.D. Thesis, Massachusetts Institute of Technology, 1990.
(5) Griffiths, J. G.; Sun, B.; Lansbury, P. A.; Griffin, R. G. In preparation.
(6) Liu, A. H.; Murray, R. C.; Dewan, J. C.; Santarsiero, B. D.; Schrock, R. R. *J. Am. Chem. Soc.* **1987**, *109*, 4282.
(7) Kubácek, P.; Hoffmann, R.; Havlas, Z. *Organometallics* **1982**, *1*, 180.
(8) Lerke, S. A.; Evans, D. H. *J. Am. Chem. Soc.* **1995**, *117*, 11768.
(9) Brookhart, M.; Green, M. L. H.; Wong, L.-L. *Prog. Inorg. Chem.* **1988**, *36*, 1.
(10) Schrock, R. R. In *Reactions of Coordinated Ligands*; Braterman, P. R., Ed.; Plenum: New York, 1986.

S0002-7863(96)00248-X CCC: $12.00 

$\sim$50 $s^{-1}$ at 25 °C), presumably via a square-pyramidal intermediate. Unfortunately, an X-ray study of $[WCp^*Me_4][PF_6]$ showed the molecule to be disordered, which is not uncommon for mono Cp* complexes; the trigonal-bipyramidal nature of the $[WCp^*Me_4]^+$ core could be confirmed, but details that might help settle the question as to why $[WCp^*Me_4]^+$ is so acidic or why the lowest energy structure is a trigonal bipyramid instead of a square pyramid could not be gleaned from the inaccurate bond lengths and angles. The solid-state NMR study of $[WCp^*Me_4][PF_6]$ reported here therefore was undertaken in order to possibly help settle some of the issues surrounding the structure and chemistry of this unusual species.

## Experimental Section

$[WCp^*(^{13}CH_3)_4][PF_6]$, $[WCp^*(^{13}CD_3)_4][PF_6]$, $[WCp^*(CD_3)_4][PF_6]$, and $[W(\eta^5\text{-}C_5Me_4Et)Me_4][PF_6]$[11] were all prepared by methods analogous to those used to prepare $[WCp^*Me_4][PF_6]$.[6]

**$^{13}$C NMR Measurements.** MAS $^{13}$C spectra of $[WCp^*(^{13}CH_3)_4][PF_6]$ and $[WCp^*(^{13}CD_3)_4][PF_6]$ were obtained on a custom-built spectrometer with a 7.6-T magnet, corresponding to a $^{13}$C resonance frequency of 79 MHz. Typically, spectra were observed using a $^{13}$C 90° pulse of length 2.5 $\mu$s and CW $^1$H decoupling during acquisition with a field strength of 100 kHz corresponding to a $^1$H 90° pulse length of 2.5 $\mu$s. All spectra shown were taken without cross polarization, although spectra obtained with cross polarization (not shown) were essentially identical. Spinning speeds were 4.0 kHz. Recycle times varied from 5 s at high temperature to 120 s at low temperature. Selective inversion-recovery was performed with a rotor-synchronized DANTE sequence with 4 cycles to selectively invert a single line, followed by a recovery delay (without $^1$H decoupling), then a $^{13}$C 90° pulse and acquisition as above. Temperatures were calibrated using the temperature-dependent $^{207}$Pb chemical shift of lead nitrate in a manner described by Bielecki.[12]

**$^2$H NMR Measurements.** Static (non-MAS) $^2$H spectra of $[WCp^*(CD_3)_4][PF_6]$ were obtained on a custom-built spectrometer with a 9.4-T magnet, corresponding to a deuterium resonance frequency of 61 MHz. Typically, spectra were observed using a quadrupole echo pulse sequence with $^2$H 90° pulse lengths of 2 $\mu$s and echo times of 30 $\mu$s. The sampling rate was 1 MHz. Recycle times varied from 3 s at high temperatures to 60 s at low temperature. $T_1$ inversion-recovery was performed with a nonselective 180° pulse of 4 $\mu$s followed by a recovery delay and a quadrupole echo sequence for observation.

**$^2$H NMR Simulations.** Deuterium NMR simulations were performed using a modified version of a program described by Wittebort et al.[13] Input parameters include the motional model (rates and geometries) and quadrupole coupling parameters. Using a given motional model, the program calculates the powder average of the motion-dependent line shape and relaxation rates for a polycrystalline sample.

**$^{13}$C NMR Simulations.** Simulations of the MAS $^{13}$C NMR line shape in the axial methyl $^{13}CH_3$ as a function of the proton hopping rate were performed using a program discussed elsewhere.[14] Input parameters include the $^1$H hopping rate, the $^1$H decoupling power (which was assumed to be 100 kHz, as described above), the $^{13}$C chemical shift tensor, the $^{13}$C$-^1$H and $^1$H$-^1$H dipole coupling constants (which were assumed to be 27 and 25 kHz, respectively, on the basis of typical values of C−H bond lengths and H−H distances in methyl groups), and the geometry of these interacting spins.

## Results

**X-ray Structural Study of $[W(\eta^5\text{-}C_5Me_4Et)Me_4][PF_6]$.** The X-ray study of $[W(\eta^5\text{-}C_5Me_5)Me_4][PF_6]$ confirmed that the overall geometry is trigonal bipyramidal with a $PF_6^-$ ion widely separated from the metal.[6] However, both the Cp* ligand and the $PF_6^-$ ion displayed a disorder that could not be resolved. Although the W atom and the four methyl groups attached to it refined comparatively well, bond lengths and angles around the metal were unreliable. Disorder is not rare for Cp* complexes, and the problem often has been circumvented by substituting $\eta^5$-$C_5Me_4Et$ for $\eta^5$-$C_5Me_5$.[15] That turned out to be the case here also.

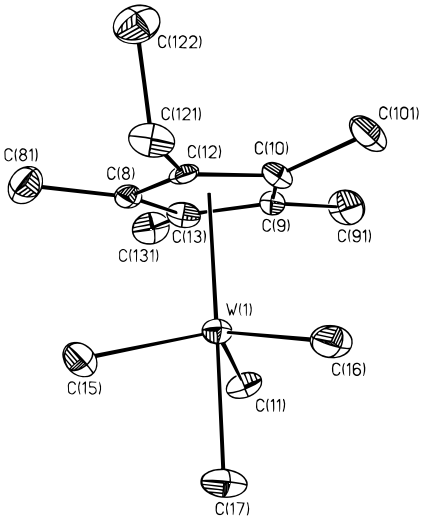


**Figure 1.** An ORTEP drawing of $[W(\eta^5\text{-}C_5Me_4Et)Me_4]^+$ (molecule 1).

**Table 1.** Selected Bond Distances (Å) and Angles (deg) for the W-Methyl Groups in $[W(\eta^5\text{-}C_5Me_4Et)Me_4][PF_6]$

| | molecule 1 | molecule 2 |
|---|---|---|
| | Distances | |
| W−C(11) | 2.132(11) | 2.143(11) |
| W−C(15) | 2.114(11) | 2.114(11) |
| W−C(16) | 2.122(11) | 2.122(10) |
| W−C(17) | 2.182(11) | 2.182(10) |
| | Angles (deg) | |
| C(15)−W−C(11) | 117.0(5) | 115.5(5) |
| C(15)−W−C(16) | 111.4(5) | 112.9(5) |
| C(16)−W−C(11) | 116.9(5) | 116.5(5) |
| C(17)−W−C(16) | 77.7(5) | 77.0(4) |
| C(17)−W−C(11) | 75.8(5) | 76.4(5) |
| C(17)−W−C(15) | 77.6(5) | 77.1(4) |

The X-ray structure of $[W(\eta^5\text{-}C_5Me_4Et)Me_4][PF_6]$ is ordered and of high quality. Two molecules are found in the unit cell along with one molecule of dichloromethane. An ORTEP drawing of the cation of molecule 1 can be found in Figure 1 and bond distances and angles for the methyl groups bound to tungsten in both cations are listed in Table 1. Bond distances between the metal and the cyclopentadienyl ligand all fall in the normal range (2.40−2.44 Å), while bond angles and other bond distances within the cyclopentadienyl ligand are also unexceptional. The four cyclopentadienyl methyl groups and the ethyl group are forced away from the metal, giving the $\eta^5$-$C_5Me_4Et$ ligand a dish shape, which is typical for penta(alkyl)-substituted cyclopentadienyl ligands in transition metal complexes. A complete list of distances and angles for both molecules can be found in the supporting information. Only the $WMe_4$ core for the two cations in the unit cell will be discussed here.

The three $W-Me_{eq}$ (C(11), C(15), C(16)) bond lengths in the two molecules are statistically the same, averaging 2.12 Å. This distance is slightly shorter than W−Me bond lengths in a variety of (mostly square pyramidal) species that contain the

(11) Green, M. L. H.; Hughes, A. K.; Popham, N. A.; Stephens, A. H. H.; Wong, L.-L. *J. Chem. Soc., Dalton Trans.* **1992**, 3077.
(12) Bielecki, A.; Burum, D. P. *J. Magn. Reson. Ser. A* **1995**, *116*, 215.
(13) Wittebort, R. J.; Olejniczak, E. T.; Griffin, R. G. *J. Chem. Phys.* **1987**, *86*, 5411.
(14) Long, J. R.; Sun, B. Q.; Bowen, A.; Griffin, R. G. *J. Am. Chem. Soc.* **1994**, *116*, 11950.
(15) See, for example: Okuda, J.; Herdtweck, E.; Herrmann, W. A. *Inorg. Chem.* **1988**, *27*, 1254.

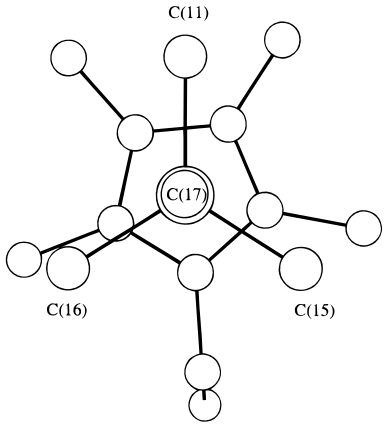


**Figure 2.** A Chem 3D view of $[W(\eta^5\text{-}C_5Me_4Et)Me_4]^+$ (molecule 1) from the axial methyl site (C(17)).

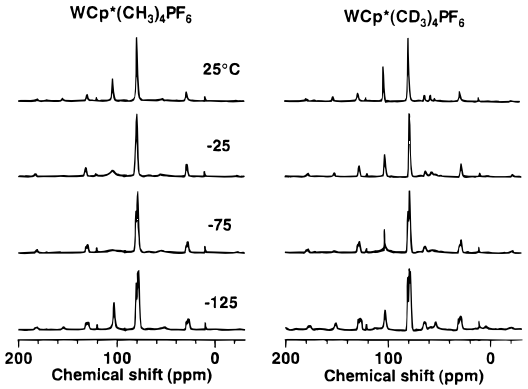


**Figure 3.** Variable-temperature MAS $^{13}C$ NMR spectra of $[WCp^*(^{13}CH_3)_4][PF_6]$ and $[WCp^*(^{13}CD_3)_4][PF_6]$ at a spinning speed of 4.0 kHz.

$Cp^*WMe_x$ ($x = 2$, or, more often, 3) core (2.19−2.24 Å).[16−20] The one instance of relatively short W−Me bonds (2.13 and 2.11 Å) is in $[WCp^*Me_2(OC_6F_5)]_2(\mu\text{-}N_2)$,[17] in which the arrangement about each metal is approximately square pyramidal. The shorter W−Me bond lengths can be rationalized on the basis of the more electron poor nature of the metal as a consequence of the presence of the electron-withdrawing perfluorophenoxide ligand. Therefore the cationic nature of $[W(\eta^5\text{-}C_5Me_4Et)Me_4]^+$ should also result in W−Me bonds that are shorter than typically found in most related neutral $WCp^*Me_x$ species. The $W-Me_{ax}$ bond length (2.18 Å) is marginally longer than $W-Me_{eq}$ bond lengths, closer to the W−Me bond lengths usually observed in $WCp^*Me_x$ species (2.19−2.24 Å). Steric repulsion between equatorial and axial methyl groups could account for the marginally longer $W-Me_{ax}$ bond length, even though there is no tungsten compound that contains a methyl group trans to a Cp* ring with which to compare the bond length found here. Steric repulsion between equatorial and axial methyl groups is likely to be exacerbated by the fact that the equatorial methyl groups are all pushed away from the cyclopentadienyl ligand, the $Me_{eq}-W-Me_{ax}$ angles deviating little from 77°. The only deviation from local 3-fold symmetry of the $WMe_4$ core is a marginally smaller value for *one* of the $Me_{eq}-W-Me_{eq}$ angles (∼112.2° average for the two molecules) versus the other two (116.5° average for the two molecules). However, as shown in a view from the bottom of molecule 1 (Figure 2), the marginally smaller angle (C(15)−W−C(16)) is the one with only one of the cyclopentadienyl carbon atoms (and its ethyl substituent) projected between the two methyl groups. Two cyclopentadienyl ring carbon atoms (with methyl substituents) in this view lie between C(11) and C(15) and between C(11) and C(16). Therefore the orientation of the cyclopentadienyl ring alone is sufficient to explain the fact that one $Me_{eq}-W-Me_{eq}$ angle is slightly smaller than the other two in the solid state.

The X-ray study is of sufficiently high quality to allow us to conclude that at least in terms of distortions of the $WC_4$ core there is no compelling evidence for any interaction between the metal and a CH bond in either an equatorial methyl group or the axial methyl group in $[W(\eta^5\text{-}C_5Me_4Et)Me_4]^+$. If we assume that the structure of a $\eta^5\text{-}C_5Me_5$ complex is virtually identical to the structure of a $\eta^5\text{-}C_5Me_4Et$ complex, an assumption that has been made by many in the past, then we can say that any such interaction in $[W(\eta^5\text{-}C_5Me_5)Me_4][PF_6]$ in the solid state is also unlikely.

**$^{13}C$ NMR Spectra of $[WCp^*Me_4][PF_6]$.** MAS $^{13}C$ NMR spectra of $[WCp^*(^{13}CH_3)_4][PF_6]$ are shown in Figure 3 at temperatures ranging from 25 to −125 °C. The isotropic axial and equatorial $^{13}CH_3$ lines are located at 105 and 80 ppm, respectively, as reported in the solution $^{13}C$ NMR study.[6] The weak lines at 122 and 11 ppm are due to the natural abundance ring and methyl carbons of the Cp* ligand, and the remaining lines are rotational sidebands. As the temperature is decreased the equatorial methyl line at 80 ppm broadens until at −125 °C it has separated into its three inequivalent components. At the same time, the axial line at 105 ppm gradually broadens without shifting, until at −58 °C it disappears into the baseline. As the temperature is further decreased the line reappears at the same frequency and narrows. This broadening of the axial $^{13}CH_3$ line is similar to that reported recently in the $^{15}N$ spectra of the $^{15}NH_3$ in alanine.[14] It is caused by interference between the $^1H$ decoupling and motion as first described by Rothwell and Waugh.[21] When the methyl motional rate is comparable to the $^1H$ decoupling nutation frequency, the two processes interfere destructively. The result is ineffective decoupling and thus a severe broadening of the resonances for nuclei that are coupled to these protons. Invocation of this mechanism is supported by the fact that when $^{13}CH_3$ is replaced by $^{13}CD_3$, in which all couplings (carbon−deuterium and deuterium−deuterium) are small and effectively removed by magic angle spinning, the axial methyl line does not exhibit this broadening, as shown in the MAS $^{13}C$ NMR spectra of $[WCp^*(^{13}CD_3)_4][PF_6]$ (Figure 3). The axial methyl line at 105 ppm disappears and reappears in the spectrum of the $CH_3$ compound, but not in that of the $CD_3$ compound. Since the $^1H$ decoupling fields that were used were typically 100 kHz, the broadening indicates methyl motional rates of approximately $10^5\ s^{-1}$ at −58 °C and approximate rates of $10^7\ s^{-1}$ at 25 °C and $10^3\ s^{-1}$ at −120 °C. Figure 4 shows a comparison of the experimental and best fit simulated[14] centerbands of the axial methyl at the indicated temperatures and rates. The $^{13}C$ chemical shift anisotropy parameters used for the axial methyl group were $\delta = -59$ ppm and $\eta = 0$, which were extracted using the method of Herzfeld and Berger from the spinning sideband intensities.[22] A tetrahedral geometry was used for all displayed simulations for the axial methyl group. We note that the simulation results are not sensitive to a specific geometry, i.e., moderate distortions of methyl tetrahedral symmetry would not produce significant deviations. These data,

(16) Liu, A. H.; O'Regan, M. B.; Finch, W. C.; Payack, J. F.; Schrock, R. R. *Inorg. Chem.* **1988**, *27*, 3574.
(17) O'Regan, M. B.; Liu, A. H.; Finch, W. C.; Schrock, R. R.; Davis, W. M. *J. Am. Chem. Soc.* **1990**, *112*, 4331.
(18) Schrock, R. R.; Kolodziej, R. M.; Liu, A. H.; Davis, W. M.; Vale, M. G. *J. Am. Chem. Soc.* **1990**, *112*, 4338.
(19) Glassman, T. E.; Liu, A. H.; Schrock, R. R. *Inorg. Chem.* **1991**, *30*, 4723.
(20) Glassman, T. E.; Vale, M. G.; Schrock, R. R.; Kol, M. *J. Am. Chem. Soc.* **1993**, *115*, 1760.
(21) Rothwell, W. P.; Waugh, J. S. *J. Chem. Phys.* **1981**, *74*, 2721.
(22) Herzfeld, J.; Berger, A. E. *J. Chem. Phys.* **1980**, *73*, 6021.

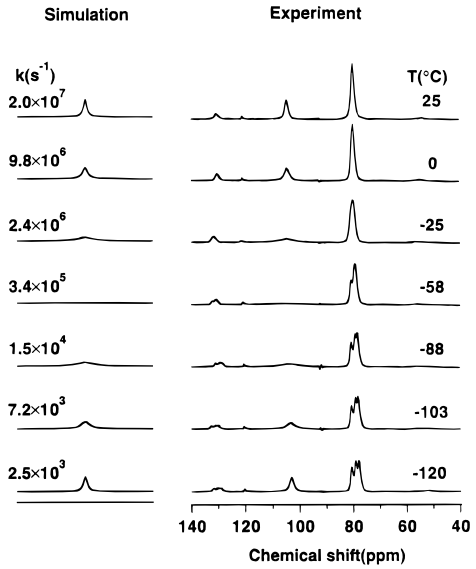


**Figure 4.** Comparison of experimental and simulated $^{13}C$ line shape of the axial methyl of $[WCp^*(^{13}CH_3)_4][PF_6]$.

along with data obtained in other experiments, are used to construct an Arrhenius plot, from which an activation energy for hopping of the axial methyl group (26.8 ± 1.7 kJ/mol, using all data; see later) is obtained.

It is appropriate at this point to clarify our terminology regarding methyl group motion. The internal motion of a methyl group may be described by several models. The common parlance of "rotation" generally suggests a free rotor moving coherently, which, in the limit of fast motion, would exhibit NMR spectra with rotational sidebands. In contrast, simple stochastic models include continuous (or free) diffusion in a constant axial potential, or discrete diffusion in a potential with two or more minima. This last type of motion is often conceptually simplified further as "hopping" from one minimum ("well") to another, which can be modeled as discrete jumps. Diffusion in a potential with three minima is easily distinguished from continuous diffusion, since in the fast limit continuous diffusion yields $^2H$ NMR relaxation spectra with no anisotropy, whereas discrete diffusion ("methyl hopping") yields significant and characteristic $T_1$ anisotropy.[13,23] In $[WCp^*Me_4]^+$ a distinct $T_1$ anisotropy is present in $^2H$ spectra. We thus use the term "methyl hopping" to indicate discrete stochastic diffusion in a potential with three minima or sites. This term is to be distinguished from the physical exchange of intact methyl groups between methyl sites, which we will call methyl exchange.

For reasons to be explained below, the rate of exchange of axial and equatorial methyl groups is of importance. Solution $^1H$ NMR studies indicated that axial and equatorial methyls exchange at a rate of ~50 $s^{-1}$ at 25 °C.[6] To ascertain these rates in the solid state, a selective inversion-recovery experiment was performed. The axial methyl was inverted with a DANTE sequence and its recovery was observed. The observed spectra at the indicated recovery times are shown in Figure 5 for $[WCp^*(^{13}CD_3)_4][PF_6]$. The intensities of the axial and equatorial methyl lines are shown as a function of recovery time at 25, 0, and −25 °C in Figure 6. The decrease in the intensity of the equatorial line as the inverted axial line recovers indicates magnetization (population) exchange. This magnetization exchange is nearly identical at the lower temperatures which indicates that in this regime, magnetization exchange is due to spin-diffusion. Such spin-diffusion exchange is dependent on the strengths of the spin couplings, which are independent of temperature. (The $^2H$ compound was used to minimize the

(23) Torchia, D. A.; Szabo, A. *J. Magn. Reson.* **1985**, *64*, 135.

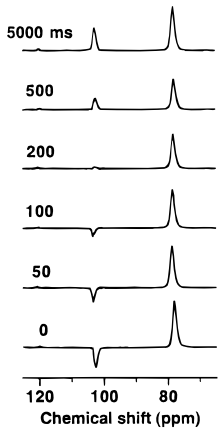


**Figure 5.** Selective inversion-recovery MAS $^{13}C$ NMR spectra of $[WCp^*(^{13}CD_3)_4][PF_6]$ at 25 °C and the recovery times indicated.

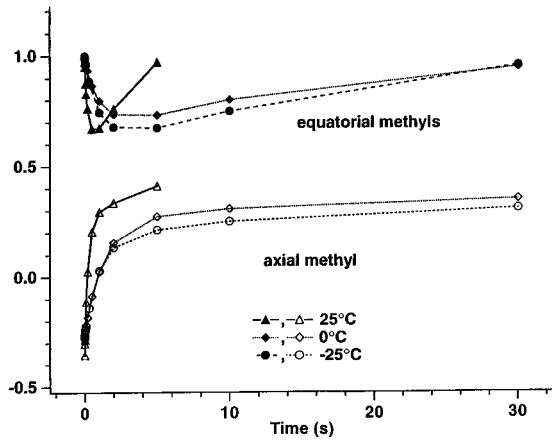


**Figure 6.** Comparison of the $^{13}C$ selective inversion-recovery of the axial and equatorial methyl lines of $[WCp^*(^{13}CD_3)_4][PF_6]$ as a function of recovery time and temperature.

effects of $^1H$-mediated spin diffusion.) In contrast, the magnetization exchange is increased at 25 °C and is therefore due in part to methyl group exchange which would likewise increase with temperature. The magnetization exchange at 25 °C is on the time scale of 0.2 to 1 s which indicates that the methyl group exchange rate is on the order of 1 to 5 $s^{-1}$. The exact methyl group exchange rate is difficult to completely separate from spin diffusion at 25 °C and is obscured completely at the lower temperatures. The existence of methyl group exchange and some knowledge of the order of magnitude of the exchange rate are sufficient for the subsequent analysis.

**$^2H$ NMR Spectra of $[WCp^*Me_4][PF_6]$.** Deuterium NMR is a well-established technique for studying molecular motions over a broad range of rates.[24] Deuterons in alkyl groups typically exhibit quadrupole splittings of 128 kHz ($(e^2Qq/h)$ = 170 kHz) in the rigid lattice limit (rate $k < 10^4$ $s^{-1}$). Quadrupole echo deuterium spectra exhibit dramatically attenuated intensities and unusual line shape features in the intermediate exchange regime ($k \sim 10^4$ $s^{-1}$ to $10^7$ $s^{-1}$). The spectra regain full intensity in the motionally narrowed fast limit ($k > 10^7$ $s^{-1}$). The $T_1$ attains a minimum (~20 ms) at rates comparable to the Larmor frequency. Deuterium $T_1$ anisotropy is highly sensitive to the geometry of the motion, and relaxation and line shape analyses of $^2H$ NMR spectra can be used for detailed examinations of molecular motion.

A $^2H$ NMR study was undertaken in order to confirm and further quantify the dynamics and the estimated rates proposed

(24) Vold, R. R.; Vold, R. L. In *Advances in Magnetic and Optical Resonance*; Warren, W. S., Ed.; Academic Press, Inc.: New York, 1991; Vol. 16, p 85.

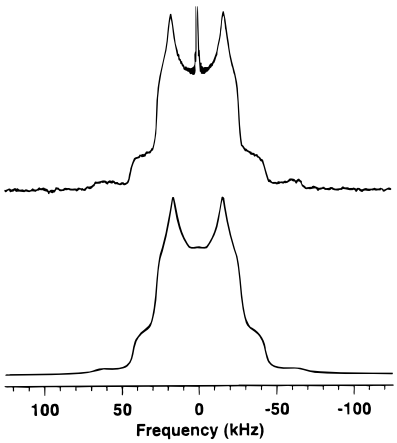


**Figure 7.** Quadrupole echo $^2$H NMR spectra of [WCp*$(CD_3)_4$][$PF_6$] at −90 °C.

on the basis of the $^{13}$C NMR spectral broadening illustrated in Figures 3 and 4. The $^2$H NMR quadrupole echo spectrum of [WCp*$(CD_3)_4$][$PF_6$] at −90 °C as well as a simulated spectrum is shown in Figure 7. Since all the methyls coordinated to tungsten are $^2$H labeled, the static powder pattern spectrum consists of the sum of the contributions from each of these. The −90 °C spectrum shows a major component with a quadrupole splitting of approximately 40 kHz and a minor component with quadrupole splittings of approximately 130 kHz. The splitting of the major component is indicative of a methyl in the fast limit ($k > 10^7$ s$^{-1}$) while the splitting of the minor component is indicative of a methyl in the slow limit ($k < 10^4$ s$^{-1}$). The relative intensities of the major and minor components are consistent with the assignment of the major component to three equatorial methyls in the fast limit and the minor component to the single axial methyl in the slow limit, as is illustrated in the simulation. The simulation confirms the general motional rates obtained from the $^{13}$C NMR data.

The $^2$H NMR line shape of the major component due to the three equatorial methyls is unusual in two ways. The line shape is significantly asymmetric with $\eta = 0.2$ and has a calculated rigid lattice ($e^2Qq/h$) value of 178 kHz. This ($e^2Qq/h$) value is slightly large for a methyl group. However, in [WCp*$(CD_3)_4$]-[$PF_6$] the transition metal may exert strong electrostatic effects, as suggested by the downfield shifted $^{13}$C resonances for both the axial and equatorial methyls. Consequently such a $^2$H quadrupole coupling constant is not extraordinary. What is more intriguing is that the major component of the *motionally narrowed* $^2$H line shape shows such a large asymmetry. The existence of similar asymmetries has been noted in other deuterated methyl compounds such as thymine,[25] hexamethylbenzene,[26] and octatrienylideneimines.[27] Theoretically, the averaging process due to motions of 3-fold (or higher) symmetry, such as a tetrahedral methyl group, results in an axially symmetric motionally narrowed line shape.[23] Several hypotheses have been presented to explain these observed asymmetries, but a consensus has not yet been achieved. Hiyama et al.[25] have presented evidence that the asymmetry is due to distortions in the electric field gradient. Specifically, in their study of thymine the asymmetry was ascribed to the presence of an electrostatic charge on the nearby exocyclic oxygen as indicated by ab initio electronic orbital calculations. Hoatson et al.[26] model their results for hexamethylbenzene as distortions in the 6-fold ring motion, whereas Wann and Harbison[27] invoke a distortion in the 3-fold geometry of the methyl itself to explain the asymmetry in octatrienylideneimines.

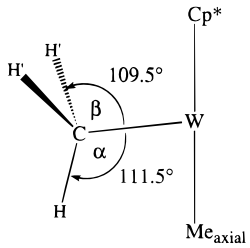


**Figure 8.** Illustration of the geometry used in the $^2$H NMR line shape simulations of the equatorial methyl groups.

As pointed out by Hoatson et al., these models make the canonical assumption that the axis of symmetry of a single deuteron EFG tensor is colinear with the CD internuclear vector, thus establishing the connection to molecular geometry. Thus, these models may equally be viewed in terms of distortions of the EFG principal axes, while the molecular geometry remains undisturbed. Nevertheless, Wann and Harbison demonstrate several cases of excellent agreement between actual measured distortions of hydrogen geometries in methyl groups and observed asymmetries. We thus discuss our analysis in terms of geometrical distortions (as in Wann and Harbison), using the following reasoning. The X-ray structure of [W(η⁵-$C_5Me_4$-Et)$Me_4$]$^+$ shows a distortion of the plane of the equatorial methyl carbons downward from the tungsten center such that the $C_{axial}$−W−$C_{equatorial}$ bond angles are ∼80°, partially as a consequence of repulsion of the methyl groups by the Cp* ligand. Bending of the equatorial methyl groups away from the Cp* ligand would suggest that the carbon−hydrogen bonds in the methyl groups also would be distorted. In addition, distortion of the methyl geometry can be readily simulated, since calculations of the motionally averaged line shapes depend explicitly on geometry. In all our simulations we have used a distortion of the methyl geometry (in the terminology of Wann and Harbison) of $\alpha = 111.5°$, $\beta = 109.5°$, and $\phi = 124°$ (where $\phi$ is the projection of the H′−C−H′ angle on a plane perpendicular to the W−C bond; see Figure 8), as opposed to the canonical values of $\alpha = 109.5°$, $\beta = 109.5°$, and $\phi = 120°$. It should be noted that this chosen geometry is independent of how the methyl group is oriented with respect to the rest of the molecule. We cannot discount the proposal that the asymmetry is due to electrostatic distortions of the EFG principal axes, which is plausible in light of the fact that [WCp*$Me_4$]$^+$ is a cation. It is certainly possible that the large asymmetry is the result of a combination of both geometric and electrostatic effects. The distorted geometric model we use is the simplest system that is consistent with both our NMR results and the X-ray structural study of [W(η⁵-$C_5Me_4$Et)$Me_4$]$^+$.

**$^2$H NMR $T_1$ Relaxation of [WCp*$(CD_3)_4$][$PF_6$].** In order to further quantify the motional model, $^2$H $T_1$ inversion-recovery measurements were performed over a range of temperatures. The contributions from the individual components are more difficult to separate at temperatures approaching 25 °C, where both equatorial and axial methyls are in the fast limit and exhibit motionally averaged line shapes of comparable breadth. Nevertheless, the $T_1$ inversion-recovery spectra at 25 °C and the simulations that best fit the spectra are shown in Figure 9. At this temperature the axial methyl hopping rate is comparable to the Larmor frequency (61 MHz) so its $T_1$ is short (∼20 ms). The hopping rate of the equatorial methyls (assumed to be the same for all three) is higher, resulting in a longer $T_1$ of several hundred milliseconds. The simulated inversion recovery spectra for these two components are shown in dashed and dotted lines,

(25) Hiyama, Y.; Roy, S.; Guo, K.; Butler, L. G.; Torchia, D. *J. Am. Chem. Soc.* **1987**, *109*, 2525.
(26) Hoatson, G. L.; Vold, R. L.; Tse, T. Y. *J. Chem. Phys.* **1994**, *100*, 4756.
(27) Wann, M.-H.; Harbison, G. S. *J. Chem. Phys.* **1994**, *101*, 231.

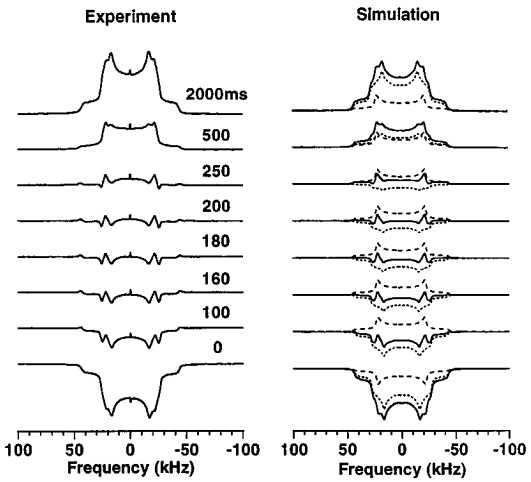


**Figure 9.** Experimental and simulated inversion-recovery $^2$H NMR spectra of [WCp*$(CD_3)_4$][$PF_6$] at 25 °C and the recovery times indicated. The simulated spectra show the individual contributions of the axial methyl (long-dashed) and equatorial methyls (short-dashed), displaying the different intrinsic relaxation times, and the sum (solid curve). The rates used in the simulations were $2.4 \times 10^{11}$ $s^{-1}$ for the equatorial methyl motion, $3.0 \times 10^7$ $s^{-1}$ for the axial methyl motion, and 1.0 $s^{-1}$ for the chemical exchange between axial and equatorial methyls.

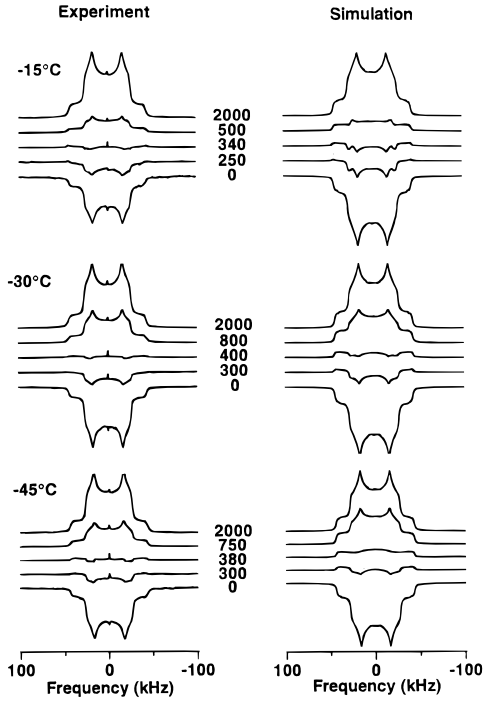


**Figure 10.** Experimental and simulated inversion-recovery $^2$H NMR spectra of [WCp*$(^{13}CD_3)_4$][$PF_6$].

along with the sum, shown as a solid line. This sum reproduces well the primary features of the experimental spectra.

The experimental and simulated spectra at several lower temperatures are shown in Figure 10. Features of interest include the attenuation of the axial component at −15 °C as its hopping rate enters the intermediate exchange regime ($k \sim 10^6$ $s^{-1}$), where quadrupole echo intensity losses are severe and the axial component therefore is invisible compared to the equatorial component. Less obvious but still significant is the fact that the average relaxation times are not monotonic. A line shape in the motionally averaged fast limit and relaxation times on the order of several hundred milliseconds corresponds to rates on the order of $10^{11}$ $s^{-1}$. In that regime the relaxation time decreases with decreasing rate, and hence decreasing temperature. However, the average $T_1$ is 300 ms at 25 °C, increasing to a maximum of 600 ms at −30 °C, then decreasing to 500 ms at −45 °C. This anomaly was too large to be ascribed to the sum of three methyls relaxing with a single time constant and one methyl relaxing with a different time constant, but can be understood by taking into consideration methyl group exchange between axial and equatorial sites. An increased rate of methyl group exchange can effectively average the relaxation times of the two components. At 25 °C, axial methyls with motional rate constants of $3.0 \times 10^7$ $s^{-1}$ relax completely in a time of roughly 60 ms. Equatorial methyls, with motional rate constants of $2.4 \times 10^{11}$ $s^{-1}$, have a relaxation time constant of approximately 600 ms, and are still inverted during the first several hundred milliseconds. If the two methyl groups exchange with a rate constant of ∼5 $s^{-1}$ or a time constant of ∼200 ms, then the methyl group that is previously unrelaxed in an equatorial site, but is now in the axial site, may now relax in the next 60 ms, leading to apparent relaxation of both methyl populations. Through such exchange, the apparent relaxation time of the intrinsically slowly relaxing equatorial component is shortened. This is an unusual situation since the two populations have significantly different $T_1$'s, and since methyl group exchange between the populations occurs with a time constant on the order of the longer of the two relaxation time constants. The $^2$H NMR simulation program was modified to account specifically for such exchange dynamics which were used in the displayed simulations. The hopping rates of the equatorial and axial methyl groups determined by $^2$H (and $^{13}$C) NMR simulations are plotted versus $1/T$ in Figure 11. The data were fit to the Arrhenius equation and yield an effective activation barrier of 10.9 ± 0.4 kJ/mol (2.6 ± 0.1 kcal/mol) for the equatorial methyl groups and 26.8 ± 1.7 kJ/mol (6.4 ± 0.4 kcal/mol) for the axial methyl group.

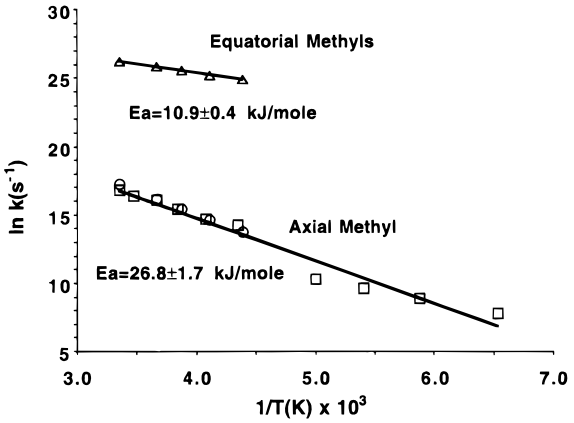


**Figure 11.** Arrhenius plot of hopping rates for the axial and equatorial methyls of [WCp*$(CH_3)_4$][$PF_6$] based on the $^{13}$C line shape simulations and the $^2$H relaxation simulations (Δ, equatorial $^2$H simulations; O, axial $^2$H simulations; □, axial $^{13}$C simulations).

## Discussion

One of the initial reasons for studying [W($\eta^5$-$C_5Me_5$)$Me_4$]$^+$ (and for determining the structure of [W($\eta^5$-$C_5Me_4Et$)$Me_4$]$^+$) was to evaluate the possibility of some interaction between a CH bond in a methyl group and the metal, an "α-agostic" interaction.[9] An α-agostic interaction could explain the enhanced acidity of certain (especially cationic) alkyl complexes of tantalum and tungsten and their tendency to form alkylidene complexes readily upon additon of a base such as $NEt_3$.[10] Agostic interactions involving $\beta$ protons in alkyl ligands are well-documented by structural and NMR methods,[9] but support for α-agostic interactions in monomeric species is slim. The only structural evidence is the neutron diffraction study of

$TiMeCl_3(Me_2PCH_2CH_2PMe_2)$,[28] while the only (solution) NMR technique that has been employed is temperature-dependent isotopic perturbation of resonance (IPR). (IPR depends on the existence of differences in bond distance potential energy profiles between agostic C−H bonds and normal C−H bonds.) IPR was employed recently[11] in order to investigate potential α-agostic interactions in several partially deuterated methyl complexes in solution, among them $TiMeCl_3(Me_2PCH_2CH_2PMe_2)$ and [W($\eta^5$-$C_5Me_4$Et)$Me_4$]$^+$. A small temperature-dependent $^1$H NMR chemical shift (∼0.14 to 0.19 ppm) of partially deuterated equatorial methyl groups in [W($\eta^5$-$C_5Me_4$Et)$Me_4$]$^+$ was measured below the point at which sharp resonances for axial and equatorial methyl groups are observed (∼253 K). Since only one of the three methyl groups could be involved in an agostic interaction at once, the "actual" chemical shift for one partially deuterated methyl group therefore was reasoned to be three times the observed shift, which would place the shift in the range observed in the osmium system originally explored by Shapley.[29] However, it was noted that the resonance for the *undeuterated* equatorial methyl groups also moves to higher field as the temperature is lowered and that "..the inherent temperature dependence of either $\delta_t$ and/or $\delta_b$ is greater than that due to the Shapley effect."[11] Yet a value for $\Delta E$ (0.84 ± 0.2 kJ mol$^{-1}$), the difference in energy between the "bridging" and "terminal" protons in the "agostic" equatorial methyl group, was extracted using the chemical shifts obtained at 273 K and assuming that the chemical shifts for terminal protons in the one "agostic" and the two "non-agostic" equatorial methyl groups were the *same*. The authors also noted that in spite of the fact that the neutron diffraction study of $TiMeCl_3(Me_2PCH_2CH_2PMe_2)$[28] shows that the methyl group is distorted toward an α-agostic form, the $^1$H NMR spectrum of $Ti(CH_2D)Cl_3$(dmpe) shows *no* evidence of isotopic perturbation that would be expected of an agostic methyl group. Therefore the authors conclude that "The absence of IPR effects on partial deuteriation is not definitive evidence for the *absence* of an agostic bond."

We have confirmed the experimental findings of Green et al. but do not believe that their interpretation of the observed IPR effect is definitive. On the basis of the discussion of the distortion of the equatorial methyl groups (as evidenced by the $^2$H line shape asymmetry), there are perhaps other reasons for temperature-dependent chemicals shifts of the magnitude observed in [W($\eta^5$-$C_5Me_5$)$Me_4$]$^+$, i.e., the observed small IPR effect in the equatorial methyl groups may be related to geometric distortion. No unambiguous low-energy CH stretch is observed in the IR spectrum of [W($\eta^5$-$C_5Me_5$)$Me_4$]$^+$ that would be consistent with an agostic interaction, and the structure of [W($\eta^5$-$C_5Me_4$Et)$Me_4$]$^+$ can be explained adequately without invoking any α-agostic interaction involving either the equatorial methyl groups or the axial methyl group. Finally, if an agostic interaction were present in a given methyl group, one might expect the hopping rate of that methyl group to be slowed compared to others. Yet we find that the *axial* methyl group hopping rate is significantly *slower* than the equatorial methyl group hopping rate. However, we cannot use the data we have obtained to argue whether an agostic interaction in an axial or equatorial methyl group is present or not. In this light it would be interesting to determine if hexamethylbenzene[26] or octatrienylideneimines[27] would also show an IPR effect. If so, then agostic interactions may be sufficient for IPR effects, though not necessary. In other words, the *presence* of IPR effects on partial deuteration, especially relatively small effects, is not definitive evidence for the *presence* of an agostic bond in all circumstances.

The barrier of 27 kJ/mol for the axial methyl presented in this study is unusually large for sterically hindered methyl group motion. Activation barriers for methyl group 3-fold hopping are typically 8−12 kJ/mol in aliphatic compounds. Large barriers have been previously measured in alanine (20 kJ/mol)[30] and *N*-acetylvaline(15 and 22 kJ/mol).[31] Precise measurements of barriers to methyl group hopping in transition metal compounds have been scarce.[32,33] Therefore we cannot comment as to the role of steric factors alone in slowing the hopping rate in transition metal compounds or to what extent the hopping rate is sensitive to the local symmetry near the methyl group in question, overall charge on the complex, overall symmetry of the complex, the nature of the other ligands present, etc. More examples of slow methyl group hopping in transition metal complexes must be uncovered before additional conclusions can be drawn. An obvious question is whether the methyl group hopping rate in [Ta($\eta^5$-$C_5H_5$)$_2Me_2$]$^+$, a species that can be readily deprotonated to give observable Ta($\eta^5$-$C_5H_5$)$_2(CH_3)(CH_2)$,[34] would also be dramatically slowed, and if so, whether that slow hopping can be ascribed only to steric factors or to an α-agostic interaction.

## Conclusions

The temperature-dependent broadening of the *axial* methyl $^{13}$C line in trigonal-bipyramidal [W($\eta^5$-$C_5Me_5$)$Me_4$]$^+$ is due to unusually slow hopping ($E_a$ = 26.8 ± 1.7 kJ/mol or 6.4 ± 0.4 kcal/mol) between the three hydrogen sites, a process that proceeds on the same time scale as the CW $^1$H decoupling periodicity. An agostic interaction of a CH bond in the axial methyl group with the metal need not be invoked to explain slow hopping. The motionally averaged line shapes for the equatorial methyl groups in [W($\eta^5$-$C_5Me_5$)$Me_4$]$^+$ were significantly asymmetric, a behavior wholly unexpected for fast limit motion. The hopping rate in the equatorial methyl groups was determined by $^2$H $T_1$ inversion-recovery measurements to be 10.9 ± 0.4 kJ/mol (2.6 ± 0.1 kcal/mol). The observed IPR effect in an equatorial methyl group could be ascribed to geometric distortion, rather than an α-agostic interaction. An X-ray study of [W($\eta^5$-$C_5Me_4$Et)$Me_4$]$^+$ provided no evidence (in terms of W−Me bond lengths or Me−W−Me bond angles) for an agostic interaction involving either the axial methyl group or the equatorial methyl groups.

**Acknowledgments.** R.R.S. thanks the National Science Foundation (currently CHE 91 22827) for research support. R.G.G. acknowledges the support of the National Institutes of Health (GM-25505, GM-23289, and RR-00995). We also thank the National Science Foundation for funds to support the purchase of a departmental Siemens SMART/CCD diffractometer.

**Supporting Information Available:** A description of X-ray data collection and structure solution and refinement, a labeled ORTEP diagram, and tables of final positional parameters, bond lengths and angles, and final thermal parameters for [W($\eta^5$-$C_5Me_4$Et)$Me_4$][$PF_6$] (7 pages). Ordering information is given on any current masthead page.

JA960248H

(28) Dawoodi, Z.; Green, M. L. H.; Mtetwa, V. S. B.; Prout, K.; Schultz, A. J.; Williams, J. M.; Koetzle, T. F. *J. Chem. Soc., Dalton Trans.* **1986**, 1629.
(29) Calvert, R. B.; Shapley, J. R. *J. Am. Chem. Soc.* **1978**, *100*, 7726.
(30) Beshah, K.; Olejniczak, E. T.; Griffin, R. G. *J. Chem. Phys.* **1987**, *86*, 4730.
(31) Beshah, K.; Griffin, R. G. *J. Magn. Reson.* **1989**, *84*, 268.
(32) Jordan, R. F.; Norton, J. R. *J. Am. Chem. Soc.* **1979**, *101*, 4853.
(33) Lafleur, D.; Huang, Y.; Gilson, D. F. R.; Butler, I. S. *J. Solid State Chem.* **1994**, *108*, 99.
(34) Schrock, R. R.; Sharp, P. R. *J. Am. Chem. Soc.* **1978**, *100*, 2389.